Design and synthesis of heteroditopic aza-thioether macrocycles for metal extraction

Mark W. Glenny,[a] Marie Lacombe,[a] Jason B. Love,[a] Alexander J. Blake,[a] Leonard F. Lindoy,[b] Robert C. Luckay,[b] Karsten Gloe,[c] Bianca Antonioli,[c] Claire Wilson[a] and Martin Schröder*[a]

Received (in Montpellier, France) 28th June 2006, Accepted 14th August 2006
First published as an Advance Article on the web 26th September 2006
DOI: 10.1039/b609180f

A series of pendant arm aza-thioether macrocycles containing hydrogen-bonding amide functionalities have been synthesised and the single crystal X-ray structures of [12]aneS_3N–CONHCOPh, [12]aneS_3N–CSNHCOPh, [12]aneS_2ON–CONHCOPh, [12]aneS_2ON–CH_2CONHCONH–^{t}Bu, [15]aneS_2ON_2–(CH_2CONHCONH–^{t}Bu)$_2$ and [15]aneS_3N_2–(CH_2CONHPh)$_2$ are presented. The structural results confirm that the majority of the macrocyclic C–S linkages adopt gauche conformations with all sulfur atoms being *exo*-orientated with respect to the macrocyclic ring, while the oxygen atoms, when present, are *endo*-orientated. The pendant arms, formed by reaction of the parent macrocycle with acyl isocyanates, are twisted from co-planarity and typically form a distorted U-shape with angles between planes formed around the carbonyl units varying from 50.81° to 68.05°. The dominant motif in these structures involves dimeric units linked through hydrogen-bonds: however, such a network is disrupted in [12]aneS_3N–CSNHCOPh by the substitution of a carbonyl unit for a thiocarbonyl unit. When more than one amide unit is present in the pendant arm, intramolecular hydrogen-bond networks are observed resulting in coplanar pendant arms and highly directional hydrogen-bonding. Inclusion of a methylene linker between the macrocycle and carbonyl function in the pendant arm inhibits intermolecular hydrogen-bond formation resulting in interaction of the amide proton with the macrocyclic nitrogen centres. A single crystal X-ray structure of [Ag([12]aneS_3N–CH_2CONH–^{t}Bu)(NO_3)] confirms binding of Ag(I) to the macrocyclic moiety with additional hydrogen-bonding [N–H···O 2.901(3) Å] between the macrocyclic pendant arm amide unit and the nitrate anion demonstrating that in the solid-state these ligands can act as heteroditopic receptors for metal salts. Overall, the solid-state structure of this complex is a one-dimensional polymer in which the Ag(I) cation is in a distorted square-pyramidal geometry with the apical sulfur donor emanating from an adjacent macrocyclic molecule. The efficacy of these ligands in competitive membrane transport and liquid–liquid metal ion extraction of Co(II), Ni(II), Cu(II), Zn(II), Cd(II), Ag(I) and Pb(II) has been assessed using selected ligands. In preliminary experiments, clear extraction and transport selectivity for Ag(I) was observed in all systems investigated, while only modest extraction of TcO_4^- was identified.

Introduction

A powerful strategy to achieve discrimination in binding and transport of metal ions is *via* the use of mixed donor ligands in which the complexing properties of the ionophore can be fine-tuned.[1] The design and synthesis of heteroditopic ionophores incorporating both cationic and anionic binding sites represents a powerful methodology for the binding, extraction and transport of metal salts.[2,3] Cooperative ion-pair binding, where complexation of a metal cation acts as a switch for selective anion binding or *vice versa* is also of interest.[4] Most commonly in these types of systems the well-established co-ordinative ability of hosts such as crown ethers and calixarenes are combined with anion receptors such as uranyls,[5] amides,[2,6] boryls[7] and zinc porphyrins.[8] However, these systems have tended to be useful for the tandem complexation of main group halides and hydrogen phosphates. We were interested in targeting transition metal ions, specifically the precious metals, with the aim of using heteroditopic molecules to bind and recover metal cations together with their associated anion(s).[3,9–11] Tasker and co-workers have used zwitterionic ionophores derived from salen incorporating both phenoxy and protonated amine centres to bind $CuSO_4$ and $NiSO_4$ salts.[3] We were interested in developing ionophores based around thioether macrocycles which are well known to co-ordinate strongly to a range of heavy and precious transition metal ions.[12] We report herein the synthesis of a series of functionalised aza-thioether and aza-oxa-thioether macrocycles incorporating peripheral hydrogen-bonding amide

[a] *School of Chemistry, University of Nottingham, University Park, UK NG7 2RD. E-mail: m.schroder@nottingham.ac.uk*
[b] *Centre for Heavy Metals Research, School of Chemistry, F11, The University of Sydney, NSW 2006, Australia*
[c] *Department of Chemistry, TU Dresden, 01062 Dresden, Germany*

groups. The parent aza-thioether macrocycles can be readily synthesised in relatively large scales and incorporate a secondary nitrogen atom as a design feature for subsequent facile derivatisation.[10,13] The new derivatives reported herein contain amide anion receptors, which were designed to fulfil several design criteria, including ease of synthesis, possible enhanced lipophilicity, and the potential for extensive hydrogen-bonding interactions.

Results and discussion

Synthesis and structural studies

Several routes were explored towards the synthesis of substituted macrocycles for use in the present study (Fig. 1). In this context the most useful were found to be the reaction of the aza-thioether macrocycles with isocyanates, isothiocyanates, chloroacylureas and benzyl halides. An advantage of using these reagents is that they are either commercially available or may be readily prepared in high yield. In a typical

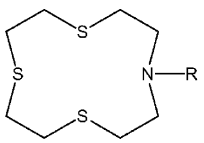

R = CONHCOPh (**1**)
CSNHCOPh (**2**)
CONHPh (**4**)
CSNHPh (**5**)
$CONHPhNO_2$-4 (**6**)
$CONHCOPhNO_2$-4 (**7**)
$CH_2CONHCONH$-tBu (**13**)
CH_2CONH-tBu (**18**)
$CH_2CONHPh$ (**20**)

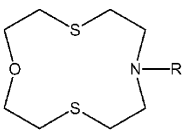

R = CONHCOPh (**3**)
$CH_2CONHCONH\,{}^tBu$ (**12**)
$CH_2CONHCONHPh$ (**17**)
$CH_2CONHPh$ (**21**)

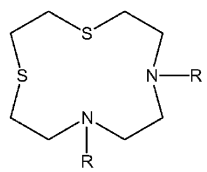

R = CONHCOPh (**8**)
CSNHCOPh (**9**)
$CONHCOPhNO_2$-4 (**10**)
$CH_2CONHCONH$-^{t}Bu (**14**)

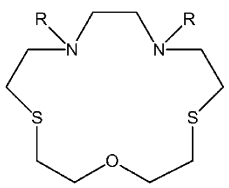

R = CONHCOPh (**11**)
$CH_2CONHCONH$-^{t}Bu (**15**)
$CH_2CONHPh$ (**22**)
H (**25**)
CH_2PhNO_2-4 (**26**)
CH_2Ph (**27**)

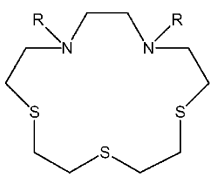

R = $CH_2CONHCONH$-^{t}Bu (**16**)
CH_2CONH-^{t}Bu (**19**)
$CH_2CONHPh$ (**23**)

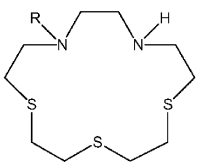

R = $CH_2CONHPh$ (**24**)

Fig. 1 Summary of ionophores prepared with numbering scheme.

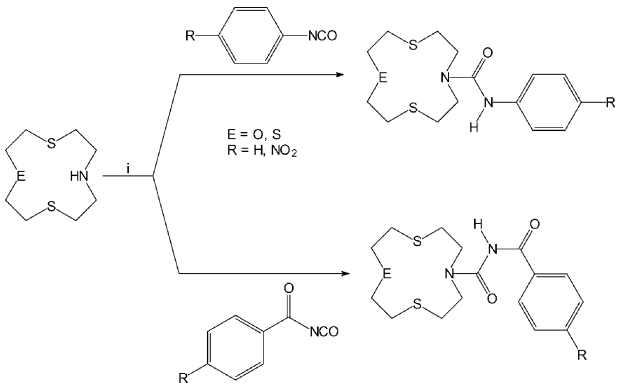

Fig. 2 Synthesis of macrocycles with pendant amide arms. (i. 1,2-dichloroethane, reflux.)

reaction, a mixture of benzoylisocyanate and [12]aneNS_3 was heated in 1,2-dichloroethane to yield the amide derivative, [12]aneS_3N–C(O)NHC(O)Ph (**1**) in high yield (Fig. 2). The ^{1}H-NMR spectrum of **1** shows the amide hydrogen resonating downfield (9.04 ppm) of the aromatic proton signals. The amide bond to the macrocyclic ring of **1** might be expected to display restricted rotation since the N–C_{arm} bond has significant double bond character; however, there is no clear evidence for this in either the ^{1}H- or ^{13}C-NMR spectra which contain sharp resonances, although some spectral overlap occurs in this region. In contrast, the NMR spectrum of [12]aneS_3N–C(S)NHC(O)Ph (**2**), prepared in a similar manner to **1** but from benzoylisothiocyanate, shows multiple resonances attributable to severely hindered rotation about the macrocyclic N–C_{arm} bond. Characterisation of both **1** (Fig. 3) and **2** (Fig. 4) by X-ray diffraction was undertaken in order to examine the effect of the amide and thioamide pendant arms on the structures of these compounds in the solid-state. In both structures the respective carbonyl or thiocarbonyl groups in the pendant arms are non–co-planar with angles between planes defined by N(1), C(9), O(1), N(2) and C(11), C(10), O(2), N(2) of 50.81° for the first and 53.11° for the second independent molecule of **1**; the angle between N(1), C(9), S(4), N(2) and C(11), C(10), O(1), N(2) is 56.50° in **2**, while the phenyl rings are also twisted from co-planarity with the

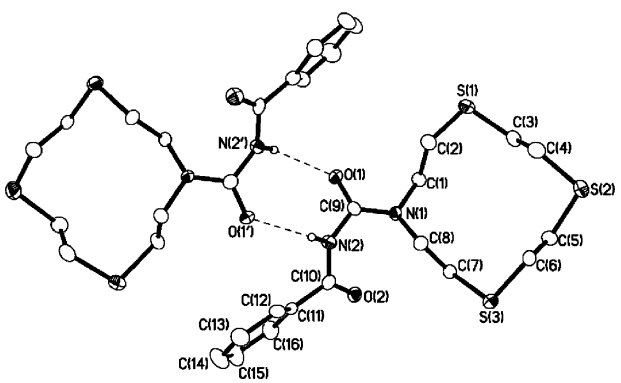

Fig. 3 X-Ray crystal structure of **1** showing intermolecular hydrogen-bonding between pendant arms. Displacement ellipsoids are drawn at 50% probability, all non-imide hydrogen atoms have been omitted for clarity.

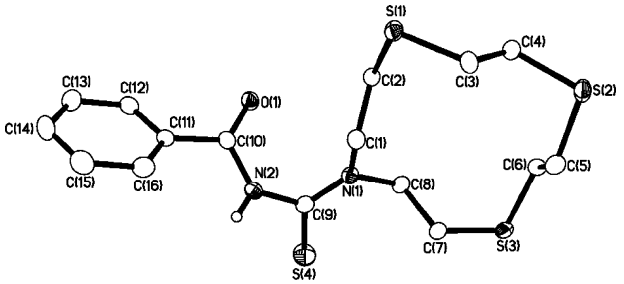

Fig. 4 X-Ray crystal structure of **2**. Displacement ellipsoids are drawn at 50% probability, all non-imide hydrogen atoms have been omitted for clarity.

adjacent carbonyl function. Unlike cyclic amides where the carbonyl functions are forced to occupy a 'W' type conformation, in these acyclic amides a range of conformations is possible. The three planar, *cis-cis*, *cis-trans*, *trans-trans*, conformations and the factors leading to their relative stability have been discussed elsewhere.[14,15]

The hydrogen-bonding network in **1** comprises dimeric units with N–H···O distances of 2.746(4) and 2.893(4) Å involving the carbonyl group closest to the macrocyclic ring [C(9)–O(1)] and the amide hydrogen on the opposing molecule. The second carbonyl unit [C(10)–O(2)] is not involved in hydrogen-bonding interactions. The hydrogen-bonding network in **2** is interesting since all H-bonds involve the more basic thioamide group and not the amide oxygen donor, with intermolecular N–H···S contacts of 3.331(2) Å.

The X-ray structure of [12]aneS_2ON–CONHCOPh (**3**, Fig. 5), formed by the reaction of [12]aneNOS_2 and benzoylisocyanate, shows an angle of 68.05° for the equivalent angle between the planes of adjacent carbonyl functions as discussed above for **1** and **2**. The common conformation found for most structurally characterised thioether macrocycles involves an *exo*-arrangement of the S-donors although an *endo*-arrangement can sometimes be favoured.[16] The tendency for an *exo*-sulfur arrangement has been attributed to the preference of C–S linkages to adopt gauche conformations, balanced with the destabilising effect of the mutual repulsion of S-lone pairs.[16] In **3** the torsion angles around the O-donor, C–O–C–C (169° and 178°), take up the favoured antiperiplanar conformation with the O-centre pointing into the ring. The S-lone pairs are directed out of the ring in the prevalent *exo*-orientation, as is the N-donor, with C–S–C–C torsion angles of −102, 80, −128 and 67°. This results in a heart-shaped structure for the macrocycle. Despite the preference for gauche torsion angles at C–S linkages in thioether macrocycles, it can be clearly seen from the angles in **3** that significant flexibility exists: at least one of the torsion angles is more properly described as being eclipsed with a neighbouring hydrogen atom. Examination of torsion angles in other crystallographically characterised thioether macrocycles[17] reveals that this phenomenon is reasonably common, and a computational study of four thioether macrocycles in the gas phase has predicted the presence of eclipsed conformations in high energy structures.[18] The situation in **3** is complicated by the presence of other heteroatoms, which are known to disrupt gauche placements through opposing influences in various segments of the macrocyclic ring. This is particularly evident when compared to the macrocyclic C–S and C–N torsion angles in **1** and **2** which are all gauche (a spread of 63.7 to 82.8° occurs for both independent molecules of **1** in the unit cell and from 66.6 to 87.7° for **2**). For **3**, hydrogen-bonded dimers are formed involving an amide hydrogen on one molecule and the carbonyl attached to the macrocycle on another, while the second carbonyl unit plays no role in hydrogen bonding. This is similar to the arrangement found in **1**.

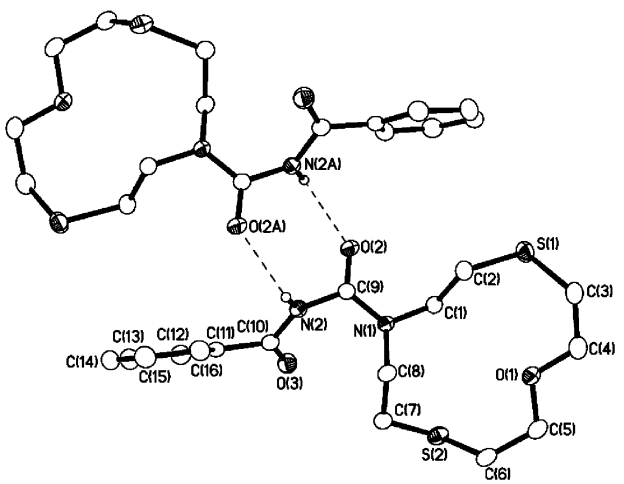

Fig. 5 X-Ray crystal structure of **3** showing intermolecular hydrogen-bonding between pendant arms. Displacement ellipsoids are drawn at 50% probability, all non-imide hydrogen atoms have been omitted for clarity.

Reaction of the aza function of the respective macrocycles with isocyanates to form amide-containing pendant arms has been generally successful, as demonstrated by the range of isocyanates and macrcocycles that we have employed (Fig. 1). When di-aza macrocycles, *e.g.* [12]aneN_2S_2, undergo reaction with two equivalents of an isocyanate, the NMR spectra of the resulting products tend to be complicated by the restricted rotation about each N–C_{arm} bond. The solubility of the resulting di-substituted products is often very low, especially for nitrophenylisocyanate derivatives and to a lesser extent for the related mono-aza macrocycles.

A particular goal was to incorporate further functionality into the pendant arms, one target being the incorporation of amino groups which are synthetically versatile. Thus, inclusion of a nitro functionality into the pendant-macrocycles (**6**, **7**, **10** and **26**) allowed the possibility of reduction to an amino group for subsequent derivatisation. Trial reduction reactions on a model compound, formed from diethylamine and 4-nitrophenylisocyanate, showed that excellent conversion to the corresponding amine was achieved using Pd/C–hydrazine hydrate[19] and lower yields with $SnCl_2$–EtOH.[20] Unfortunately, all attempts using these and other reagents with the present macrocyclic derivatives almost exclusively resulted in cleavage of the pendant arm, which was rapid in acidic media. Initial metal complexation experiments also indicated that the N–C_{arm} bond is prone to cleavage in the presence of many metal salts.

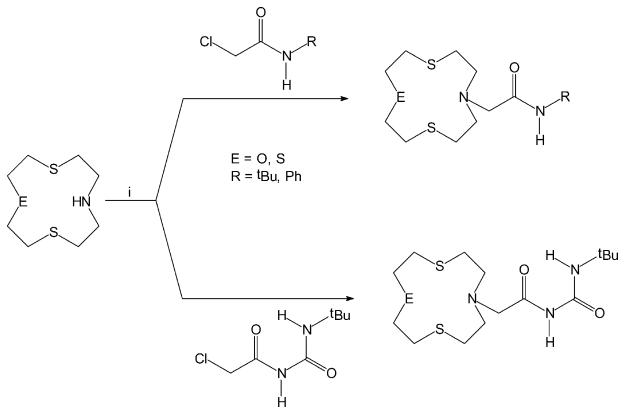

Fig. 6 Synthesis of pendant arm macrocycles *via* chloroacylamides. (i. K_2CO_3, MeCN, reflux.)

In order to avoid such decomposition, the pendant arms were modified by introducing a methylene linker between the macrocycle and the amide moieties. A versatile reaction involving chloroacylureas and chloroacylamides was used to introduce these pendant arms onto the macrocycle (Fig. 6). For example, reaction of 12]aneNOS$_2$, 1-*tert*-butyl-3-(chloroacetyl)urea and K_2CO_3 in MeCN afforded the pendant macrocycle, [12]aneS$_2$ON–CH$_2$CONHCONH–^{t}Bu (**12**), in 60% yield after aqueous workup. The presence of the pendant arm was confirmed by ^{1}H-NMR spectroscopy, which showed a shift in macrocyclic ring resonances compared to the metal-free ionophore and the presence of two additional broad signals at δ 8.21 and 9.32 assigned to the amide protons of the pendant arm. These latter signals were shown to shift considerably in the presence of a diamagnetic metal ion such as Ag(I).

In order to examine the effect of introducing the methylene linker into its pendant arm, a crystal structure determination of **12** was undertaken (Fig. 7). The arrangement of the macrocyclic ring is generally the same as that found in **3**, with the N and S-donors exodentate and the O-donor endodentate: however, the torsion angles around the sulfur donors in **12** are all gauche (57.15–67.53°). The main differences occur in the pendant arm since in **12** an extra amide function is present. The pendant arm is well set-up for intramolecular hydrogen-bonding and the structure shows a nearly planar pendant arm

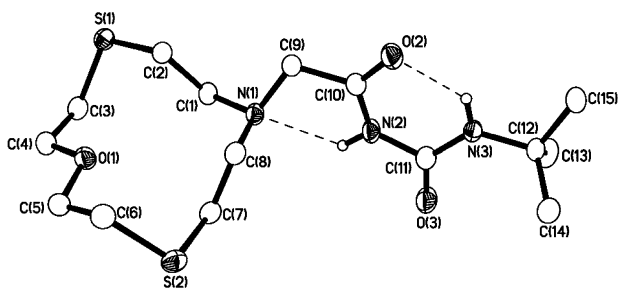

Fig. 7 X-Ray crystal structure of **12** showing the intramolecular hydrogen-bonding in the pendant arm. Displacement ellipsoids are drawn at 50% probability, all non-imide hydrogen atoms have been omitted for clarity.

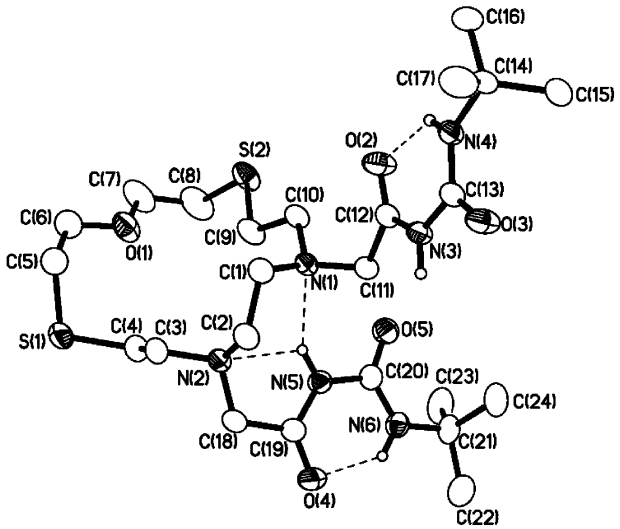

Fig. 8 X-Ray crystal structure of **15** showing the high degree of intramolecular hydrogen-bonding. Displacement ellipsoids are drawn at 50% probability, all non-amide hydrogen atoms have been omitted for clarity.

[angle between planes defined by C(9), C(10), O(2), N(2) and N(3), C(11), O(3), N(2) is 8.82°] with N(2)–H(2A)···N(1) and N(3)–H(2A)···O(2) distances of 2.6927(18) and 2.7168(18) Å, respectively.[21]

Compounds **13–24** incorporating amide and urea moieties in the pendant arm(s) were prepared in an analogous manner to that of **12**. The di-aza macrocycles undergo substitution at one or both nitrogen atoms depending on the stoichiometry of the reactants employed. For example, [15]aneS$_2$ON$_2$–(CH$_2$CONHCONH–^{t}Bu)$_2$ (**15**)[10] was isolated in 67% yield after workup. The pendant arms appear equivalent in the NMR spectra, although in concentrated solutions the signals attributed to the *tert*-butyl groups in the ^{1}H-NMR spectrum are split (δ 1.34 and 1.35 ppm), with the amide protons observed at 8.19 and 9.19 ppm. In the ^{13}C-NMR spectra of both **12** and **15** the methylene units directly bound to the ether oxygen donor are observed downfield of the other signals at 74.34 and 73.00 ppm, respectively. The latter compound also exhibits two infrared bands at 1552 and 1715 cm^{-1} attributable to the ν(CO) modes of the carbonyls in the pendant arms.

The crystal structure of [12]aneS$_2$ON$_2$–(CH$_2$CONHCONH–^{t}Bu)$_2$ **15** was obtained in order to examine the consequences of adding two urea moieties onto the macrocycle (Fig. 8).[10] The sulfur and nitrogen donors in **15** are exodentate while the oxygen donor takes up its normal endodentate arrangement with anti conformations about the C–O bonds [−176.2(3)° and 177.9(3)°]. There are three gauche C–S–C–C torsion angles [74.5(2)°,82.4(3)° and 82.8(3)°] and one anti conformation [177.4(2)°], consistent with the preference for these conformations in thioether macrocycles.[16] As for the urea pendant arm in **12**, the carbonyl units in the pendant arms of **15** are also coplanar [angle between planes defined by: C(11)–C(12)–O(2)–N(3) and N(4), C(13), O(3), N(3) is 5.04°; C(18), C(19), O(4), N(5) and N(6), C(20), O(5), N(5) is 1.68°] with a complex network of both intramolecular and

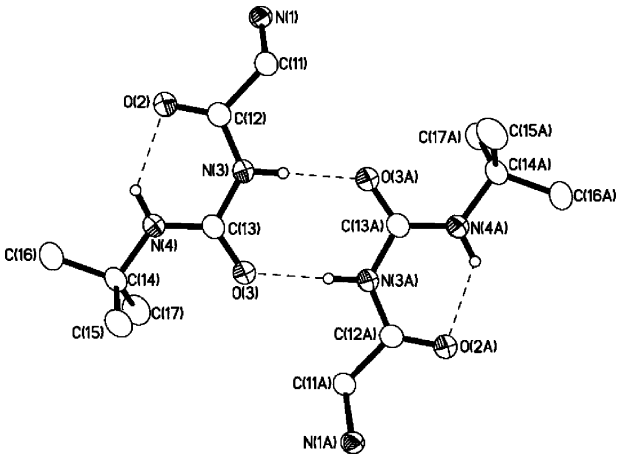

Fig. 9 View showing the intermolecular hydrogen-bonding between pendant arms in **15**. Displacement ellipsoids are drawn at 50% probability, all non-amide hydrogen atoms have been omitted for clarity.

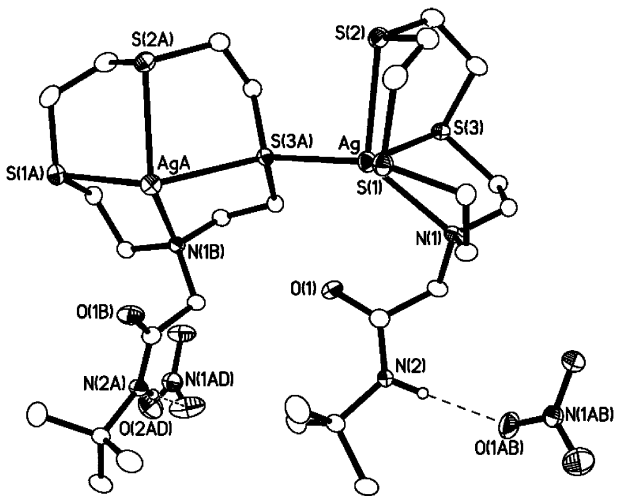

Fig. 11 View of structure of [Ag(**18**)(NO_3)] showing the intermolecular hydrogen-bonding between macrocycle pendant arm and nitrate anion. Displacement ellipsoids are drawn at 50% probability, all non-imide hydrogen atoms have been omitted for clarity.

intermolecular hydrogen-bonding being present. The resultant structure is made up of hydrogen-bonded dimers bridged through one pendant arm [N(3)–H(3)···O(3)], which is also involved in an intramolecular interaction [N(4)–H(4N)···O(2)] (Fig. 8). The other pendant arm is only involved in intramolecular hydrogen-bonding involving the amide nearest to the macrocycle and the macrocyclic nitrogen atoms; the outermost amide [N(6)–H(6)] interacts with the carbonyl oxygen [O(4)] of the innermost amide unit (Fig. 9). This leaves the outermost carbonyl oxygen atom [O(5)] free and taking no part in any strong hydrogen-bonding interactions.

In contrast, the crystal structure of [15]aneS_3N_2–($CH_2CONHPh)_2$ (**23**) (Fig. 10), which contains two amide functionalities rather than two urea functions, shows the pendant arms extending on either side of the plane of the macrocycle which leaves no potential for hydrogen-bonding between the arms. Both amide units are involved in hydrogen-bonds with the macrocyclic nitrogen centres, while, as in **15**, the carbonyl oxygen atoms are not involved in hydrogen-bonding interactions with a nearest contact of over 5 Å. The C–C–S–C torsion angles in the macrocyclic ring yield a mixture of gauche and anti arrangements which may be a

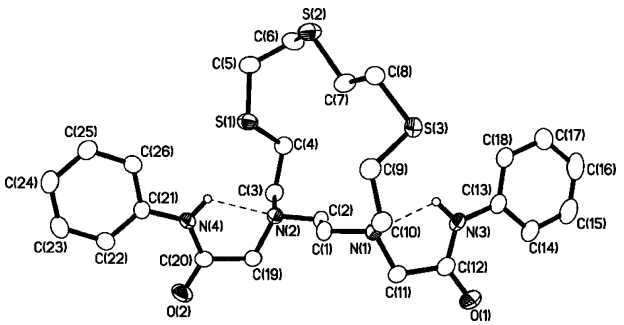

Fig. 10 X-Ray crystal structure of **23** showing the intramolecular hydrogen-bonding. Displacement ellipsoids are drawn at 50% probability, all non-amide hydrogen atoms have been omitted for clarity.

reflection of the odd number of atoms in the ring; however, it is significant that no highly unfavoured conformations are present.

We were also able to selectively substitute only one of the macrocyclic nitrogen atoms in the di-aza macrocycles. Thus, slow addition of one equivalent of *N*-phenyl-2-chloroacetamide in MeCN to a mixture of K_2CO_3 and [15]aneN_2S_3 in MeCN at 50°C results in formation of [15]aneS_3N_2–$CH_2CONHPh$ (**24**) in 43% isolated yield. The resonance attributed to the amide hydrogen appears at δ 9.71 ppm in the ^{1}H-NMR spectrum, considerably shifted downfield from that found in the analogous disubstituted species (δ 9.29 ppm). This is probably a result of inductive effects from hydrogen-bonding interactions between the macrocyclic nitrogen atom and the amide oxygen. In all other species containing the phenylacetamide arm, except that derived from [12]aneNOS_2 (**21**), this signal appears in the region δ 9.3–9.4 ppm. The effect of the electron donating ability of the *tert*-butyl group over that of the phenyl group is also noticeable in the position of the amide hydrogen resonance for **18–23**. All phenylacetamide derivatives have this resonance at δ 9.29 or above, while in the *tert*-butylacetamide derivatives this signal appears at much higher field (δ 7.22 for **18**; δ 7.06 for **19**).

Complexation studies

A preliminary investigation into the solid-state structures of these ligands with selected metal salts has proved encouraging. The single-crystal X-ray structure of [Ag(**18**)(NO_3)] (Fig. 11) demonstrates that relatively strong hydrogen-bonding interactions occur between the amide hydrogen atom and a nitrate oxygen atom [N(2)H(2A)···O(1A) 2.02 Å, N(2)···O(1A) 2.901(3) Å, ∠N(2)–H(2A)···O(1A) 178°]. The Ag(I) ion is bound to four sulfur atoms, three from one macrocycle and one from an adjacent macrocycle, and one N-donor. Overall, the co-ordination geometry is distorted square-pyramidal with the apical position occupied by the sulfur donor from the

adjacent macrocycle [S(3A)], with the resulting structure being a one-dimensional *zig-zag* polymer. Each macrocyclic cationic moiety is bridged to the next by the Ag–S(3A) bond [2.5349(8) Å] which is also the shortest of the four Ag–S bond distances, the remaining bond lengths being 2.6082(8), 2.7299(8) and 2.7153(9) Å for Ag–S(1), Ag–S(2) and Ag–S(3), respectively, while the Ag–N(1) bond length is 2.490(2) Å.

Polymeric structures are known for the Ag(I) complexes of thioether macrocycles, and these often involve exocyclic binding of the Ag(I) ion.[22,23] The co-ordination chemistry of the Ag(I) complexes of [9]aneS$_3$, [15]aneS$_5$ and [18]aneS$_6$ has been investigated previously and the structures of $[Ag([9]aneS_3)_2]^+$ and $[Ag([18]aneS_6)]^+$ reported.[24] It has been demonstrated that the structure of the $[Ag([15]aneS_5)]^+$ cation is significantly altered in the presence of different anions.[25] In the structure of the PF_6^- complex, a [4 + 1] co-ordination geometry, similar to that observed in the structure of [Ag(**18**)(NO$_3$)], was observed, with four donors from one macrocycle and a further donor from an adjacent macrocycle forming the co-ordination sphere. In $[Ag([15]aneS_5)]PF_6$, however, the intermolecular Ag–S bond distance is the longest. Comparison of the Ag–S distances in structurally characterised Ag–thioether macrocycle complexes shows that the Ag–S distance is highly variable and depends on a range of factors such as the co-ordination geometry adopted, the nature of crystal packing forces, the size of macrocycle and the nature of the anion. In the structure of [Ag(**18**)(NO$_3$)], the Ag–S distances lie at the upper end of the observed bond distance range. The macrocyclic geometry in the latter complex maintains the square shape found in other structures containing [12]aneNS$_3$; however, the donor atoms sacrifice their preferred corner positions and becomes part of a 'side', each of which is made up of runs of gauche–anti-gauche torsion angles. The positions of both ν(NH) and ν(CO) stretching vibrations in the infra-red spectrum of the complex are both shifted to higher frequency compared to the free ligand. We interpret this as being a result of significant changes in the hydrogen-bonding network due both to new ligand-nitrate interactions as well as disruption of the hydrogen-bonding pattern found in the free ligand. The ^{1}H-NMR spectrum of [Ag(**18**)(NO$_3$)] in d$_3$-MeCN shows that the signal attributed to the amide hydrogen is shifted upfield (δ 6.53) from that of the free ligand (δ 7.18 for **18** in d$_3$-MeCN). This shift is in the opposite direction from that usually associated with hydrogen-bonding interactions;[26] however, strong solvation of the cationic moiety very likely perturbs the hydrogen-bonding present in the solid-state structure. This is not entirely unexpected since the nitrate anion is not known as an especially strong hydrogen-bond acceptor[27] and the ligand contains only one hydrogen-bond donor. The signals attributed to the macrocyclic methylene units collapse into a broad singlet in the ^{1}H-NMR spectrum of the complex, suggesting a high degree of flexibility or fluxionality in the macrocyclic co-ordination.

The solution behaviour of **13** with Ag(I) salts was investigated by ^{1}H-NMR spectroscopy (Table 1). Addition of AgNO$_3$ to a solution of **13** in MeCN leads initially to an upfield shift for the N(15)–H proton from δ_H 9.01 in **13** to δ_H 8.65 on addition of 0.4 equivalents of AgNO$_3$. This upfield shift reflects the breaking of the internal H-bonding in free **13** on complexation to Ag(I) (Fig. 12). On further addition of AgNO$_3$, this resonance shows the expected downfield shift to δ_H 8.85 reflecting H-bonding of the acylurea arm to the nitrate anion as confirmed by the crystal structure of [Ag(**13**)(NO$_3$)].[9] Further addition of ^{n}Bu$_4$NNO$_3$ leads to further downfield shifts for the N(15)–H resonance (to δ_H 9.39, 9.55 and 9.65 on addition of 1, 2 and 3 equivalents of ^{n}Bu$_4$NNO$_3$, respectively) consistent with anion binding in solution (Table 1). Significantly, addition of ^{n}Bu$_4$NNO$_3$ to **13** does not shift the N(15)–H resonance; therefore, anion binding to **13** can only occur once cation binding within the macrocyclic cavity and concomitant cleavage of the internal H-bonding takes place, thus affording an element of cooperativity to this system. Thus, once the internal hydrogen-bond is broken by complexation of the ionophore by Ag(I), the central urea proton is freed to interact with anions in solution as confirmed by the downfield shift of this proton resonance on addition of NO_3^-.

Table 1 Data for ^{1}H-NMR titration of (**13**) with AgNO$_3$ and *n*-Bu$_4$NNO$_3$ carried out in d^3-MeCN. Total volume 0.4 mL: 0.25 mL L (0.071 mmol mL^{-1}) and portions of 0.071 mmol mL^{-1} AgNO$_3$ (0.2 eq, 0.4 eq, 0.6 eq and 1 eq) followed by solvent to make up to 0.4 mL volume. After 1 eq was reached, *n*-Bu$_4$NNO$_3$ was added in portions of 1 equiv. (entries 6–8)

Entry	Equiv. Ag$^+$	Equiv. *n*-Bu$_4$NNO$_3$	δ NH$_{central}$	δ NH$_{terminal}$
1	0.0	0	9.01	8.23
2	0.2	0	8.75	8.15
3	0.4	0	8.65	8.09
4	0.6	0	8.73	8.09
5	1.0	0	8.85	8.12
6	1.0	1	9.39	8.15
7	1.0	2	9.55	8.15
8	1.0	3	9.65	8.16

Membrane transport

Competitive mixed metal transport experiments (water–chloroform–water) employed an organic phase containing the ionophore (chosen from **14–16**, **20**) at 1×10^{-3} mol dm^{-3}. The aqueous source phase contained equimolar concentrations (each 1×10^{-2} mol dm^{-3}) of Co(II), Ni(II), Cu(II), Zn(II), Cd(II), Ag(I) and Pb(II) nitrate. Transport experiments were performed over 24 h against a back gradient of protons, maintained by buffering the source and receiving phases at pH 4.9 and 3.0, respectively. A common feature of all four studies based on **14–16** and **20** is that, within experimental error, sole transport selectivity for Ag(I) was observed (Table 2) under the conditions employed.

Transport efficiency/selectivity across bulk liquid membranes has long been known to be influenced by a range of often interdependent factors.[28] For example, slow kinetics and/or thermodynamic stabilities that are either too low to permit uptake of a metal into the organic phase, or too high to

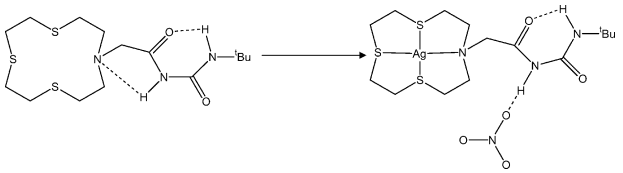

Fig. 12 Binding of AgNO$_3$ to **13**.

Table 2 Transport flux data for Ag(I) from seven-metal competitive transport across a bulk chloroform membrane employing **14–16** and **20** as ionophores (25 °C)[ab]

Ionophore	Ag(I) J/mol per 24 h[c]
14	159
15	82
16	147
20	54

[a] Values are the mean from duplicate experiments. [b] The corresponding J values for Co(II), Ni(II), Cu(II), Zn(II), Cd(II) and Pb(II) were all 0 (within experimental error). [c] All J values are $\times 10^{-7}$.

allow its loss to the receiving phase, will all inhibit transport efficiency and also affect selectivity. Because of the possible interplay of subtleties such as these, it is often difficult to analyse in detail observed transport behaviour. Although this situation pertains to the present study, it is still possible to note the following observations. Although **15** and **16** differ only by the change of one donor in the macrocyclic ring (from oxygen to sulfur), the substituted S_3N_2 derivative **16** yields a significantly higher flux for Ag(I) transport, presumably reflecting the expected higher affinity of its donor set for Ag(I) relative to the OS_2N_2-donor set of **15**. A comparable transport rate to that for **16** was found for the smaller macrocyclic derivative, **14**, showing that the additional oxygen donor in **15** (relative to **14**) in fact leads to a reduction in transport efficiency. The remaining compound, **20**, differs from the other three macrocyclic derivatives in that it incorporates a S_3N-donor set and contains only one pendant arm with a single amide functionality: it shows the poorest Ag(I) transport rate.

Liquid–liquid extraction studies

The new thia-aza crown compounds were also tested as extractants for liquid–liquid extraction of a series of different metal ions using an extraction system based upon metal salt–picric acid–buffer–H_2O/ligand–$CHCl_3$. Fig. 13 shows an overview of the extraction behaviour of the ligands studied towards Ag(I) at comparable experimental conditions. Consistent with the membrane transport studies above, the thia-aza crowns show a high affinity for Ag(I) and extract it almost quantitatively even at low ligand concentrations. Conversion of secondary amines to tertiary ones has no marked effect on

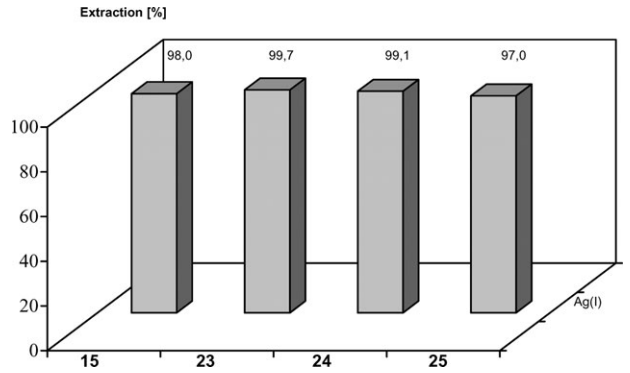

Fig. 13 Extraction of Ag(I) with pendant aza-thioethers **15**, **23**, **24** and **25**. [$AgNO_3$] = 1×10^{-4} M; pH = 5.2 (MES/NaOH buffer); [ligand] = 1×10^{-3} M in $CHCl_3$; [HPic] = 5×10^{-3} M.

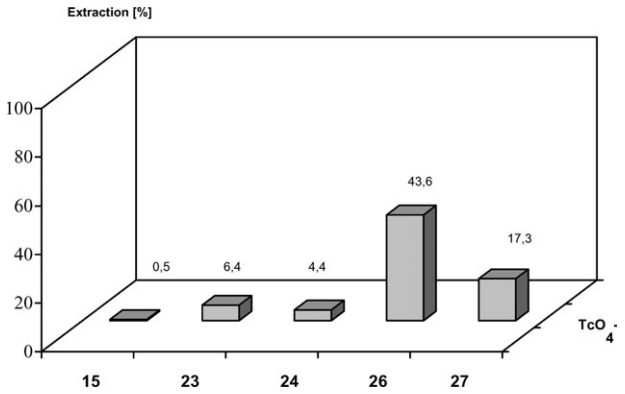

Fig. 14 Extraction of pertechnetate with pendant aza-thioethers **15**, **23**, **24**, **26** and **27**. [$NaTcO_4$] = 1×10^{-4} M; pH = 7.4 (HEPES/NaOH buffer); [ligand] = 1×10^{-3} M in $CHCl_3$.

the overall extraction behaviour under the conditions employed. Unfortunately, because of the high distribution ratios with the low applied ligand concentrations employed [2.5×10^{-4} –1.5×10^{-3} M], no information could be obtained about the composition of the extracted complexes from these experiments, although the single crystal X-ray structure of the 1 : 1 complex [Ag(**25**)(SCN)] has been reported previously and shows a solid-state co-ordination pattern that involves binding to all macrocyclic donor atoms along with a sulfur from the SCN^- ligand.[29] The stability of selected metal complexes with unsubstituted macrocycles employing mixed S_2ON_2-donor systems (including **25**) has also been reported[30] and confirms that such species show strong affinity for Ag(I) [and Cu(II)] relative to the other five transition and post-transition metal ions investigated.

Additional experiments were performed involving extraction from an aqueous source phase buffered at pH 5.2 and containing equimolar concentrations of Co(II), Ni(II), Cu(II), Zn(II), Cd(II) and Pb(II) [$> c_{M(NO_3)_2} = 1 \times 10^{-4}$ M] into a $CHCl_3$ phase incorporating ligand **25** ($c_{ligand} = 5 \times 10^{-3}$ M). This ligand shows only high extraction of Pb(II) (55%) under the conditions used here. Very low extraction levels were observed for other divalent transition metal ions, even for Ni(II), which has been shown to form a metal complex of composition [Ni(**25**)(NO_3)](NO_3) in the solid-state.[31] However, the five-fold higher ligand concentration used in this experiment, in comparison with the Ag(I) extraction by **25** confirms the pronounced preference for Ag(I) by these types of ionophores.

In addition to the above cation extraction studies, the solvent extraction behaviour of the ligands **15**, **23**, **24**, **26**, and **27** was also examined towards the TcO_4^- anion. We wished to probe whether **15**, **23** and **24** incorporating hydrogen-bonding side arms would afford a pronounced interaction with the anion. However, as shown in Fig. 14, the ligands **15**, **23** and **24** show only a very weak extraction of this oxoanion into the organic phase whereas higher extraction was observed for the benzyl and nitrobenzyl substituted ligands **26** and **27**. At the pH 7.4 employed for these experiments, it is expected that each of the ligands be present in its protonated form.[32] It thus appears that the higher lipophilicity present in **26** and **27**

relative to the amide-containing species **15**, **23**, and **24** dominates in this case and more than compensates for any tendency for the pendant arm functional groups in the latter systems to assist in anion uptake.

Conclusions

We have prepared in good yield a range of derivatised macrocycles where the pendant arm(s) contain potential hydrogen-bonding moieties comprising urea and amide functions. We envisage that these and related systems will find applications as selective metal salt extractants from, for example, dilute waste streams for the recovery of toxic and/or precious metals. Reaction of the parent macrocycles with a range of substrates has been investigated and the solid-state structures examined. The structures demonstrate that hydrogen-bonding involving the pendant arms is strong and, where there is more than one amide N–H unit, intramolecular hydrogen-bonding is the dominant influence controlling the conformations of the pendant arms. The majority of the donor atoms in the macrocycles were found to be exo-dentate in the solid-state, but NMR spectral data suggest flexibility in the macrocyclic rings in solution. The crystal structure of [Ag(**18**)(NO_3)] demonstrates that in the solid-state there is significant hydrogen-bonding between the macrocyclic amide arm and the nitrate anion, indicating that these systems may act as heteroditopic receptors for metal salts. The hydrogen-bonding network appears to be disrupted in acetonitrile solution where strong competitive solvation of the cationic moiety probably inhibits any interaction with the anion. Membrane and liquid–liquid extraction experiments have shown that these systems are highly selective for Ag(I) over a range of other metal ions.

Experimental

Materials and methods

All reagents and solvents were purchased from commercial sources and were used as received unless stated otherwise. Aza-thioether macrocycles were prepared according to the literature.[9,10,13] Benzoylisocyanate was prepared according to the literature procedure.[33] 4-Nitrobenzoylisocyanate was prepared in a similar fashion to that of benzoyl isocyanate using toluene as the solvent. 1-*tert*-Butyl-3-(chloroacetyl)urea and 1-phenyl-3-(chloroacetyl)urea were prepared by heating at reflux *tert*-butylurea or phenylurea with chloroacetylchloride in benzene. *N*-*tert*-Butyl-2-chloroacetamide and *N*-phenyl-2-chloroacetamide were prepared by adding chloroacetylchloride slowly to excess *tert*-butylamine or aniline respectively in toluene at 0 °C. Elemental analyses (C, H, N) were carried out by the by the Analytical Department of the School of Chemistry, University of Nottingham. ^{1}H-NMR and ^{13}C-NMR spectra were recorded on a Bruker AX300 FT-NMR spectrometer. Chemical shifts are referenced with respect to the residual protio solvent. Mass spectra were recorded on a Finnigan MAT TSQ-700 at the EPSRC National Service, University of Wales, Swansea.

Membrane transport

The transport experiments employed a concentric cell design in which the aqueous source phase (10 cm^3) and receiving phase (30 cm^3) were separated by a chloroform phase (50 cm^3). Details of the cell design have been reported elsewhere.[34] In each experiment all three phases were stirred separately at 10 rpm using stirring paddles for the receiving phase and propellers for the source and organic phases. Each paddle or propeller was coupled to a single (geared) synchronous motor, and the cell was enclosed by a water jacket and thermostatted at 25 °C. The aqueous source phase consisted of a sodium acetate–acetic acid buffer solution (pH 4.9 ± 0.1) containing an equimolar mixture of the metal ions, each at a concentration of 10^{-2} mol dm^{-3}. The chloroform phase contained the macrocycle at 10^{-3} mol dm^{-3}. The receiving phase consisted of a buffer solution of sodium formate–formic acid (pH 3.0 ± 0.1). All transport runs were terminated after 24 h and atomic absorption spectroscopy was used to determine the amount of each metal ion transported into the receiving phase during this period (using a Varian Spectra AA-800 spectrometer). The transport results are quoted as the average values obtained from duplicate runs; transport fluxes (*J* values) are in mol per 24 h and represent mean values measured over 24 h. *J* values equal to or less than $\sim 15 \times 10^{-7}$ mol per 24 h are zero within experimental error and were ignored in the analysis of the results.

Liquid–liquid solvent extraction

The liquid–liquid extraction experiments were performed at 23 ± 1°C in microcentrifuge tubes (2 mL) by means of mechanical shaking. The phase ratio $V_{(org)} : V_{(w)}$ was 1 : 1 (0.5 mL each). A shaking time of 30 min was chosen because in all cases the extraction equilibrium was reached during this period. After extraction, all samples were centrifuged and the phases separated. The metal concentration in both phases was determined using γ-radiation measurements of ^{110m}Ag radioisotopes in a NaI(Tl) scintillation counter (Cobra II/Canberra-Packard). For the competitive extraction experiments the metal concentration in the aqueous phase was determined by ICP-OES spectroscopy (Optima 3000/Perkin Elmer) according to standard conditions (viewing height: 9 mm, Ar plasma gas flow: 15.0 l min^{-1}, Ar auxiliary gas flow: 0.5 l min^{-1}, Ar nebulizer gas flow: 0.8 l min^{-1}; solution uptake rate: 0.1 ml min^{-1}; wavelengths-Ag: 328.068 nm; Cd: 214.438 nm; Co: 228.616 nm; Ni: 231.604 nm; Cu: 324.754 nm; Pd: 340.458 nm; Pb: 220.353 nm and Zn: 202.548 nm, integration time: 60 s each). The determination of the anion concentration in both phases was carried out radiometrically by β-radiation measurements of ^{99}Tc in a liquid scintillation counter (LS 6000 LL/Beckman).

Syntheses

[12]aneS$_3$N–CONHCOPh (1). To a solution of [12]aneNS$_3$ (0.47 g, 2.10 mmol) in 1,2-dichloroethane (25 mL) was added benzoylisocyanate (0.37 g, 2.52 mmol) with the formation of white precipitate. The mixture was heated at reflux for 1 h and the white precipitate filtered, washed with dichloromethane, hexane and then dried under reduced pressure to afford 0.58 g

(75%) of white powder. Anal. calc. for $C_{16}H_{22}N_2O_2S_3$: C, 51.86; H, 5.98; N, 7.56%. Found: C, 51.69; H, 5.85; N, 7.50%. ^{1}H-NMR ($CDCl_3$): δ (ppm) = 2.92 (m, 8H, CH_2), 2.98 (m, 4H, CH_2), 3.62 (m, 4H, CH), 7.48 (t, 2H, Ph), 7.55 (t, 1H, Ph), 7.88 (d, 2H, Ph), 9.04 (s, 1H, NH). ^{13}C-NMR ($CDCl_3$): δ (ppm) = 28.37 (CH_2), 29.90 (CH_2), 31.73 (CH_2), 49.63 (CH_2), 127.78 (CH), 128.77 (CH), 132.79 (CH), 133.19 (C_{quat}), 153.96 (CO), 166.18 (CO). IR (cm^{-1}) 3186 (νNH), 1709 (νCO), 1651 (νCO). FAB$^+$-MS m/z ($C_{16}H_{22}N_2O_2S_3$, 370): 371 (M + H$^+$).

[12]aneS$_3$N–CSNHCOPh (2). Using the same procedure as outlined for the preparation of **1**, [12]aneNS$_3$ (0.27 g, 1.21 mmol) and benzoyl isothiocyanate (0.17 mL, 1.27 mmol) afforded 0.30 g (64%) of the product as a pale yellow crystalline solid after concentration and slow cooling. Anal. calc. for $C_{16}H_{22}N_2OS_4$: C, 49.71, H, 5.74; N, 7.25%. Found: C, 49.01; H, 5.63; N, 7.01%. ^{1}H-NMR ($CDCl_3$): δ (ppm) = 2.81 (s, 8H, CH_2), 3.06 (m, 4H, CH_2), 3.82 (s, br, 2H, CH), 4.18 (s, br, 2H, CH), 7.50 (t, 2H, Ph), 7.62 (t, 1H, Ph), 7.86 (d, 2H, Ph), 8.35 (s, 1H, NH). ^{13}C-NMR ($CDCl_3$): δ (ppm) = 25.43 (CH_2), 26.04 (CH_2), 31.37 (CH_2), 51.46 (CH_2), 52.14 (CH_2), 127.83 (CH), 129.00 (CH), 132.24 (CH), 133.26 (C_{quat}), 163.99 (CO), 181.39 (CS). IR (cm^{-1}) 3326 (νNH), 1689 (νCO), 1522 (νCS). FAB$^+$-MS m/z ($C_{16}H_{22}N_2OS_4$, 386): 387 (M + H$^+$).

[12]aneS$_2$ON–CONHCOPh (3). To a solution of [12]aneNOS$_2$ (0.177 g, 0.854 mmol) in dichloromethane (15 mL) was added benzoylisocyanate (0.126 g, 0.854 mmol) and the mixture stirred at room temperature for 30 minutes after which time the solvent was removed. The resulting waxy solid was recrystallised from dichloromethane-diethyl ether to give 0.18 g (60%) of the product as a white crystalline solid. Anal. calc. for $C_{16}H_{22}N_2O_3S_2$: C, 54.21; H, 6.26; N, 7.90%. Found: C, 53.97; H, 6.26; N, 7.76%. ^{1}H NMR ($CDCl_3$): δ (ppm) = 2.78 (m, 4H, CH_2), 2.98 (m, 4H, CH_2), 3.75 (m, 8H, CH), 7.46 (t, 2H, Ph), 7.56 (t, 1H, Ph), 7.81 (d, 2H, Ph), 8.10 (s, 1H, NH). ^{13}C NMR ($CDCl_3$): δ (ppm) = 31.02 (CH_2), 32.83 (CH_2), 73.60 (CH_2), 77.20 (CH_2), 127.76 (CH), 128.68 (CH), 132.62 (CH), 133.20 (C_{quat}), 153.49 (CO), 166.63 (CO). IR (cm^{-1}) 3190 (νNH), 1688 (νCO), 1651 (νCO). FAB$^+$-MS m/z ($C_{16}H_{22}N_2O_3S_2$, 354): 355 (M + H$^+$).

[12]aneS$_3$N–CONHPh (4). Using the same procedure as outlined for the preparation of **1**, [12]aneNS$_3$ (0.050 g, 0.224 mmol) and phenylisocyanate (0.027 g, 0.227 mmol) afforded 0.067 g (87%) of the product as a white solid. Anal. calc. for $C_{15}H_{22}N_2OS_3$: C, 52.59, H, 6.47; N, 8.18%. Found: C, 52.44; H, 6.19; N, 7.74%. ^{1}H NMR ($CDCl_3$): δ (ppm) = 2.77–3.01 (m, 12H, CH_2), 3.62 (m, 4H, CH_2), 7.07 (t, 1H, Ph), 7.28 (t, 2H, Ph), 7.41 (d, 2H, Ph), 8.25 (s, 1H, NH). ^{13}C NMR ($CDCl_3$): δ (ppm) = 30.31 (CH_2), 30.39 (CH_2), 33.29 (CH_2), 52.18 (CH_2), 119.51 (CH), 123.00 (CH), 129.01 (CH), 139.03 (C_{quat}), 156.69 (CO). IR (cm^{-1}) 3279 (νNH), 1640 (νCO). EI-MS m/z ($C_{15}H_{22}N_2OS_3$, 342): 342 (M$^{+\bullet}$).

[12]aneS$_3$N–CSNHPh (5). Using the same procedure as outlined for the preparation of **1**, [12]aneNS$_3$ (0.052 g, 0.233 mmol) and phenylisothiocyanate (0.032 g, 0.237 mmol) afforded 0.071 g (85%) of the product as a white solid. Anal. calc. for $C_{15}H_{22}N_2S_4$: C, 50.24, H, 6.18; N, 7.81%. Found: C, 50.06; H, 5.76; N, 7.72%. ^{1}H-NMR ($CDCl_3$): δ (ppm) = 2.80–3.13 (m, 12H, CH_2), 3.99 (m, 4H, CH_2), 7.21–7.52 (m, 5H, Ph), 9.02 (s, 1H, NH). ^{13}C-NMR ($CDCl_3$): δ (ppm) = 29.50 (CH_2), 30.44 (CH_2), 32.97 (br, CH_2), 55.13 (CH_2), 125.24 (CH), 125.73 (CH), 128.77 (CH), 139.79 (C_{quat}), 184.02 (CS). IR (cm^{-1}) 3192 (νNH), 1525 (νCS). FAB$^+$-MS m/z ($C_{15}H_{22}N_2S_4$, 358): 359 (M + H$^+$).

[12]aneS$_3$N–CONHPhNO$_2$-4 (6). Using the same procedure as outlined for the preparation of **1** in toluene, [12]aneNS$_3$ (0.154 g, 0.689 mmol) and 4-nitrophenylisocyanate (0.113 g, 0.689 mmol) afforded 0.22 g (82%) of the product as an off-white solid after concentration and cooling. Anal. calc. for $C_{15}H_{21}N_3O_3S_3$: C, 46.49, H, 5.46; N, 10.84%. Found: C, 46.51; H, 5.43; N, 10.57%. ^{1}H-NMR ($CDCl_3$): δ (ppm) = 2.84–3.04 (m, 12H, CH_2), 3.65 (m, 4H, CH_2), 7.56 (d, 2H, Ph), 8.19 (d, 2H, Ph), 9.01 (s, 1H, NH). FAB$^+$-MS m/z ($C_{15}H_{21}N_3O_3S_3$, 387): 388 (M + H$^+$).

[12]aneS$_3$N–CONHCOPhNO$_2$-4 (7). Using the same procedure as outlined for the preparation of **1**, [12]aneNS$_3$ (0.125 g, 0.560 mmol) and 4-nitrobenzoylisocyanate (0.107 g, 0.560 mmol) afforded 0.14 g (60%) of product as a brown solid. Further product was obtained by concentrating the solution. The product was sparingly soluble in common solvents. Anal. calc. for $C_{16}H_{21}N_3O_4S_3$: C, 46.25; H, 5.09; N, 10.11%. Found: C, 45.70; H, 4.85; N, 10.16%. ^{1}H-NMR ($CDCl_3$): δ (ppm) = 2.91 (m, 12H, CH_2), 3.65 (m, 4H, CH_2), 8.02 (d, 2H, Ph), 8.32 (d, 2H, Ph), 9.55 (s, 1H, NH). IR (cm^{-1}) 3205 (νNH), 1703 (νCO), 1652 (νCO). FAB$^+$-MS m/z ($C_{16}H_{21}N_3O_4S_3$, 415): 416 (M + H$^+$).

[12]aneS$_2$N$_2$–(CONHCOPh)$_2$ (8). Using the same procedure as outlined for the preparation of **1**, [12]aneN$_2$S$_2$ (0.18 g, 0.872 mmol) and benzoylisocyanate (0.257 g, 1.74 mmol) afforded 0.43 g (100%) of the very poorly soluble product as a white solid. Anal. calc. for $C_{24}H_{28}N_4O_4S_2$: C, 57.58; H, 5.64; N, 11.19%. Found: C, 56.24; H, 5.61; N, 10.80%. ^{1}H-NMR (C_6D_6): δ (ppm) = 2.77 (s, 4H, CH_2), 2.91 (t, 4H, CH_2), 3.60 (m, 4H, CH_2), 3.89 (s, 4H, CH_2), 7.39–7.64 (m, 10H), 8.25 (s, 2H). IR (cm^{-1}) 3243 (νNH), 1700 (νCO), 1651 (νCO). FAB$^+$-MS m/z ($C_{24}H_{28}N_4O_4S_2$, 500): 501 (M + H$^+$).

[12]aneS$_2$N$_2$–(CSNHCOPh)$_2$ (9). Using the same procedure as outlined for the preparation of **1**, [12]aneN$_2$S$_2$ (0.107 g, 0.518 mmol) and benzoylisothiocyanate (0.14 mL, 1.04 mmol) afforded 0.179 g (65%) of product as an insoluble white solid. Anal. calc. for $C_{24}H_{28}N_4O_2S_4$: C, 54.11; H, 5.30; N, 10.52%. Found: C, 53.54; H, 5.22; N, 10.40%. Due to the very low solubility of the sample, no NMR data were obtained. IR (cm^{-1}) 3350 (νNH), 3287 (νNH), 1684 (νCO), 1668 (νCO), 1527 (νCS). FAB$^+$-MS m/z ($C_{24}H_{28}N_4O_4S_2$, 532): 533 (M + H$^+$).

[12]aneS$_2$N$_2$–(CONHCOPhNO$_2$-4)$_2$ (10). Using the same procedure as outlined for the preparation of **1**, [12]aneN$_2$S$_2$ (0.158 g, 0.766 mmol) and 4-nitrobenzoylisocyanate (0.294 g, 1.53 mmol) afforded 0.221 g (49%) of product as a brown solid. Further product was obtained by concentrating the solution. The product was sparingly soluble in common solvents. Anal. calc. for $C_{24}H_{26}N_6O_8S_2$: C, 48.81; H, 4.44;

N, 14.23%. Found: C, 48.18; H, 4.45; N, 13.86%. IR (cm^{-1}) 3209 (νNH), 1700 (νCO), 1651 (νCO). FAB^+-MS m/z ($C_{24}H_{26}N_6O_8S_2$, 590): 591 ($M + H^+$).

[15]aneS_2ON_2–(CONHCOPh)$_2$ (11). Using the same procedure as outlined for the preparation of **1**, [15]aneN_2OS_2 (0.273 g, 1.09 mmol) and benzoylisocyanate (0.321 g, 2.18 mmol) afforded 0.58 g (98%) of the product after crystallisation from the reaction mixture by trituration with hexane. Anal. calc. for $C_{26}H_{32}N_4O_5S_2$: C, 57.33; H, 5.92; N, 10.29%. Found: C, 57.58; H, 5.96; N, 9.68%. ^{1}H-NMR ($CDCl_3$): δ (ppm) = 2.79 (m, 4H, CH_2), 3.01 (m, br, 4H, CH_2), 3.63 (m, 4H, CH), 3.77 (m, 8H, CH), 7.46 (m, 6H, Ph), 7.81 (t, 4H, Ph), 9.05 (s, 2H, NH). ^{13}C-NMR ($CDCl_3$): δ (ppm) = 31.17 (CH_2), 31.97 (CH_2), 43.41 (CH_2), 49.55 (CH_2), 72.12 (CH_2), 127.29, 128.09 (CH), 128.39 (CH), 132.46 (CH), 132.84 (C_{quat}), 133.24 (C_{quat}), 154.00 (br, CO), 166.98 (CO). IR (cm^{-1}) 3232 (νNH), 1713 (νCO), 1652 (νCO). FAB^+-MS m/z ($C_{26}H_{32}N_4O_5S_2$, 544): 545 ($M + H^+$).

[12]aneS_2ON–CH_2CONHCONH–^{t}Bu (12). To a suspension of K_2CO_3 (0.33 g, 2.39 mmol), and KI (0.63 g) in CH_3CN (30 mL) was added [12]aneNOS_2 (0.33 g, 1.59 mmol) and 1-*tert*-butyl-3-(chloroacetyl)urea (0.31 g, 1.59 mmol) and the mixture heated at reflux for 3 h. The solvent was removed and the resulting solid extracted with dichloromethane and washed with water, brine and finally dried over $MgSO_4$. After filtration and removing the solvent the product was obtained as white solid (0.35 g, 60%) which was recrystallised from methanol. Anal. calc. for $C_{15}H_{29}N_3O_3S_2 \cdot H_2O$, C, 47.22; H, 8.14; N, 11.01% Found: C, 47.58; H, 7.78; N, 10.55%. ^{1}H-NMR ($CDCl_3$): δ (ppm) 1.37 (s, 9H, CMe_3), 2.72 (m, 4H, CH_2), 2.84 (m, 8H, CH_2), 3.76 (m, 4H, CH_2), 3.21 (s, 2H, CH_2), 8.21 (br, s, 1H, NH), 9.32 (br, s, 1H, NH). ^{13}C-NMR ($CDCl_3$): δ (ppm) = 28.86 (CMe_3), 29.10 (CH_2), 30.86 (CH_2), 50.69 (CMe_3), 52.58 (CH_2), 59.68 (CH_2), 74.34 (CH_2), 151.09 (CO), 172.94 (CO). IR (cm^{-1}) 3250 (νNH), 1716 (νCO), 1652 (νCO). FAB^+-MS m/z ($C_{15}H_{29}N_3O_3S_2$, 363): 364 ($M + H^+$).

[12]aneS_3N–CH_2CONHCONH–^{t}Bu (13). To a suspension of K_2CO_3 (1.60 g, 11.5 mmol), and KI (5 mg) in CH_3CN (50 mL) was added [12]aneNS_3 (1.46 g, 6.54 mmol) and 1-*tert*-butyl-3-(chloroacetyl)urea (1.26 g, 6.54 mmol) and the mixture heated at reflux for 2.5 h. The solvent was removed and the resulting solid extracted with dichloromethane, concentrated and triturated with diethyl ether to afford 0.159 g (64%) of the product as a white powder after isolation by filtration, washing with diethyl ether and drying under reduced pressure. Anal. calc. for $C_{15}H_{29}N_3O_2S_3$, C, 47.46; H, 7.70; N, 11.07%. Found: C, 47.13; H, 7.49; N, 10.91%. ^{1}H-NMR ($CDCl_3$): δ (ppm) 1.39 (s, 9H, CMe_3), 2.67 (m, 4H, CH_2), 2.78 (m, 4H, CH_2), 2.83 (s, 8H, CH_2), 3.18 (s, 2H, CH_2), 8.16 (br, s, 1H, NH), 8.98 (br, s, 1H, NH). FAB^+-MS m/z ($C_{15}H_{29}N_3O_2S_3$, 379): 380 ($M + H^+$).

[12]aneS_2N_2–(CH_2CONHCONH–^{t}Bu)$_2$ (14). Using the same procedure as outlined for the preparation of **12**, [12]aneN_2S_2 (0.27 g, 1.31 mmol) and 1-*tert*-butyl-3-(chloroacetyl)urea (0.50 g, 2.62 mmol) afforded 0.39 g (57%) of the product as a pale-yellow solid after drying under reduced pressure. Anal. calc. for $C_{22}H_{42}N_6O_4S_2 \cdot CH_2Cl_2$, C, 48.16; H, 7.72; N, 14.98%. Found: C, 48.26; H, 7.68; N, 14.89%. ^{1}H-NMR ($CDCl_3$): δ (ppm) 1.38 (s, 18H, CMe_3), 2.67–2.95 (m, 16H, CH_2), 3.19 (s, 4H, CH_2), 8.18 (br, s, 2H, NH), 9.12 (br, s, 2H, NH). ^{13}C-NMR ($CDCl_3$): δ (ppm) = 28.89 (CMe_3), 31.33 (CH_2), 50.83 (CH_2), 52.26 (CH_2), 53.35 (CMe_3), 54.28 (CH_2), 58.59 (CH_2), 74.34 (CH_2), 151.89 (CO), 172.09 (CO). FAB^+-MS m/z ($C_{22}H_{42}N_6O_4S_2$, 518): 519 ($M + H^+$).

[12]aneS_2ON_2–(CH_2CONHCONH–^{t}Bu)$_2$ (15). Using the same procedure as outlined for the preparation of **12**, [15]aneN_2OS_2 (0.945 g, 3.78 mmol) and 1-*tert*-butyl-3-(chloroacetyl)urea (1.45 g, 7.55 mmol) afforded 1.49 g (67%) of the product as white solid after drying under reduced pressure. Anal. calc. for $C_{24}H_{46}N_6O_5S_2$, C, 51.22; H, 8.24; N, 14.93%. Found: C, 50.88; H, 8.12; N, 14.52%. ^{1}H-NMR ($CDCl_3$): δ (ppm) 1.34 and 1.35 (s, 18H, CMe_3), 2.79 (m, 16H, CH_2), 3.17 (s, 4H, CH_2), 3.70 (m, 4H, CH_2), 8.19 (br, s, 2H, NH), 9.19 (br, s, 2H, NH). ^{13}C-NMR ($CDCl_3$): δ (ppm) = 28.80 (CMe_3), 30.09 (CH_2), 31.87 (CH_2), 50.70 (CMe_3), 51.99 (CH_2), 55.33 (CH_2), 59.36 (CH_2), 73.00 (CH_2), 151.20 (CO), 172.48 (CO). IR (cm^{-1}) 3289 br (νNH), 1715 (νCO), 1552 (νCO). FAB^+-MS m/z ($C_{24}H_{46}N_6O_5S_2$, 562): 563 ($M + H^+$).

[15]aneS_3N_2–(CH_2CONHCONH–^{t}Bu)$_2$ (16). Using the same procedure as outlined for the preparation of **12**, [15]aneN_2S_3 (0.46 g, 1.74 mmol) and 1-*tert*-butyl-3-(chloroacetyl)urea (0.67 g, 3.48 mmol) afforded 0.66 g (66%) of the product as a white solid after chromatography on silica-60 (dichloromethane–methanol 10 : 1 eluent) and drying under reduced pressure. Large crystals were obtained by recrystallisation from 1,2-dichloroethane/hexane. Anal. calc. for $C_{24}H_{46}N_6O_4S_3$, C, 49.80; H, 8.01; N, 14.52%. Found: C, 49.79; H, 7.99; N, 14.43%. ^{1}H-NMR ($CDCl_3$): δ (ppm) 1.36 (s, 18H, CMe_3), 2.81 (m, 20H, CH_2), 3.22 (s, 4H, CH_2), 8.19 (br, s, 2H, NH), 9.29 (br, s, 2H, NH). ^{13}C-NMR ($CDCl_3$): δ (ppm) = 28.81 (CMe_3), 29.96 (CH_2), 32.54 (CH_2), 32.83 (CH_2), 50.75 (CMe_3), 52.76 (CH_2), 55.36 (CH_2), 58.64 (CH_2), 151.29 (CO), 172.41 (CO). IR (cm^{-1}) 3287, 3232 (νNH), 1712 (νCO), 1550 (νCO). FAB^+-MS m/z ($C_{24}H_{46}N_6O_4S_3$, 578): 579 ($M + H^+$).

[12]aneS_2ON–CH_2CONHCONHPh (17). Using the same procedure as outlined for the preparation of **12**, [12]aneNOS_2 (0.268 g, 1.29 mmol) and 1-phenyl-3-(chloroacetyl)urea (0.275 g, 1.29 mmol) afforded 0.66 g (66%) of the product as an orange solid after chromatography on silica-60 (dichloromethane–methanol 20 : 1 eluent) and drying under reduced pressure. Anal. calc. for $C_{17}H_{25}N_3O_3S_2$, C, 53.24; H, 6.57; N, 10.96%. Found: C, 52.79; H, 6.18; N, 10.61%. ^{1}H-NMR ($CDCl_3$): δ (ppm) 2.75 (m, 4H, CH_2), 2.93 (m, 8H, CH_2), 3.32 (s, 2H, CH_2), 3.81 (m, 4H, CH_2), 7.09 (t, 1H, Ph), 7.32 (t, 2H, Ph), 7.53 (d, 2H, Ph), 9.83 (br, s, 1H, NH), 10.35 (br, s, 1H, NH). ^{13}C-NMR ($CDCl_3$): δ (ppm) = 29.36 (CH_2), 30.85 (CH_2), 52.75 (CH_2), 59.57 (CH_2), 73.98 (CH_2), 120.02 (C_{quat}), 123.96 (CH), 128.78 (CH), 137.18 (C_{quat}), 149.87 (CO), 173.48 (CO). IR (cm^{-1}) 3239 (νNH), 1712 (νCO), 1683 (νCO). FAB^+-MS m/z ($C_{17}H_{25}N_3O_3S_2$, 383): 384 ($M + H^+$).

[12]aneS$_3$N–CH$_2$CONH–^{t}Bu (18). Using the same procedure as outlined for the preparation of **12**, [12]aneNS$_3$ (0.0498 g, 0.424 mmol) and *N*-*tert*-butyl-2-chloroacetamide (0.0635 g, 0.424 mmol) afforded 0.13 g (91%) of the product as a white crystalline solid. An analytically pure sample was obtained by recrystallisation from a dichloromethane–hexane mixture. Anal. calc. for $C_{14}H_{28}N_2OS_3$, C, 49.96; H, 8.38; N, 8.32%. Found: C, 49.64; H, 8.44; N, 8.33%. ^{1}H NMR ($CDCl_3$): δ (ppm) 1.38 (s, 9H, CMe_3), 2.69 (m, 8H, CH_2), 2.83 (m, 8H, CH_2), 2.96 (s, 2H, CH_2), 7.22 (br, s, 1H, NH).%. ^{1}H-NMR (d^3-MeCN): δ (ppm) 1.35 (s, 9H, CMe_3), 2.67 (s, br, 8H, CH_2), 2.78 (s, br, 8H, CH_2), 2.88 (s, 2H, CH_2), 7.18 (br, s, 1H, NH). ^{13}C-NMR ($CDCl_3$): δ (ppm) = 27.31 (CH_2), 28.36 (CH_2), 28.72 (CMe_3), 29.50 (CH_2), 50.94 (CMe_3), 53.05 (CH_2), 59.26 (CH_2), 169.36 (CO). IR (cm^{-1}) 3252 (νNH), 3079 (νNH), 1646 (νCO), 1572 (νCO). FAB$^+$-MS *m*/*z* ($C_{14}H_{28}N_2OS_3$, 336): 337 (M + H$^+$).

[15]aneS$_3$N$_2$–(CH$_2$CONH–^{t}Bu)$_2$ (19). Using the same procedure as outlined for the preparation of **12**, [15]aneN$_2$S$_3$ (0.0763 g, 0.286 mmol) and *N*-*tert*-butyl-2-chloroacetamide (0.086 g, 0.573 mmol) afforded 0.12 g (85%) of the product as a white wax. After chromatography on silica-60 (dichloromethane–methanol 10 : 1 eluent) and drying under reduced pressure, the product obtained appeared pure by NMR spectroscopy. Anal. calc. for $C_{22}H_{44}N_4O_2S_3 \cdot CH_3OH$, C, 52.04; H, 9.22; N, 10.68% Found: C, 52.56; H, 8.71; N, 10.09%. ^{1}H-NMR ($CDCl_3$): δ (ppm) 1.31 (s, 18H, CMe_3), 2.62–2.80 (m, 20H, CH_2), 2.94 (s, 4H, CH_2), 7.06 (br, s, 2H, NH). ^{13}C-NMR ($CDCl_3$): δ (ppm) = 28.70 (CMe_3), 30.40 (CH_2), 32.83 (CH_2), 50.67 (CMe_3), 52.28 (CH_2), 54.98 (CH_2), 60.15 (CH_2), 169.50 (CO). FAB$^+$-MS *m*/*z* ($C_{22}H_{44}N_4O_2S_3$, 492): 493 (M + H$^+$).

[12]aneS$_3$N–CH$_2$CONHPh (20). Using the same procedure as outlined for the preparation of **12**, [12]aneNS$_3$ (0.133 g, 0.595 mmol) and *N*-phenyl-2-chloroacetamide (0.101 g, 0.595 mmol) afforded 0.17 g (80%) of the product as pale yellow wax after chromatography on silica-60 (dichloromethane–methanol 40 : 1 eluent) and drying under reduced pressure. Anal. calc. for $C_{16}H_{24}N_2OS_3$, C, 53.89; H, 6.78; N, 7.86%. Found: C, 54.00; H, 6.53; N, 7.65%. ^{1}H-NMR ($CDCl_3$): δ (ppm) 2.64–2.84 (m, 16H, CH_2), 3.17 (s, 2H, CH_2), 7.07 (t, 1H, Ph), 7.30 (t, 2H, Ph), 7.67 (d, 2H, Ph), 9.41 (br, s, 1H, NH). ^{13}C-NMR ($CDCl_3$): δ (ppm) = 27.52 (CH_2), 28.35 (CH_2), 29.52 (CH_2), 58.66 (CH_2), 119.35 (C_{quat}), 123.96 (CH), 128.73 (CH), 137.59 (C_{quat}), 168.32 (CO). IR (cm^{-1}) 3225 (νNH), 1685 (νCO), 1601 (νCO). FAB$^+$-MS *m*/*z* ($C_{16}H_{24}N_2OS_3$, 356): 357 (M + H$^+$).

[12]aneS$_2$ON–CH$_2$CONHPh (21). Using the same procedure as outlined for the preparation of **12**, [12]aneNOS$_2$ (0.158 g, 0.762 mmol) and *N*-phenyl-2-chloroacetamide (0.129 g, 0.762 mmol) afforded 0.18 g (70%) of the product as pale yellow wax after chromatography on silica-60 (dichloromethane –methanol 12 : 1 eluent) and drying under reduced pressure. Anal. calc. for $C_{16}H_{24}N_2O_2S_2$, C, 56.44; H, 7.10; N, 8.23%. Found: C, 57.59; H, 7.20; N, 8.09%. ^{1}H-NMR ($CDCl_3$): δ (ppm) 2.75 (m, 4H, CH_2), 2.80–2.96 (m, 8H, CH_2), 3.26 (s, 2H, CH_2), 3.78 (m, 4H, CH_2), 7.10 (t, 1H, Ph), 7.31 (t, 2H, Ph), 7.71 (d, 2H, Ph), 9.78 (br, s, 1H, NH). ^{13}C-NMR ($CDCl_3$): δ (ppm) = 30.68 (CH_2), 31.13 (CH_2), 53.19 (CH_2), 60.05 (CH_2), 73.61 (CH), 119.43 (C_{quat}), 123.84 (CH), 128.74 (CH), 137.92 (C_{quat}), 169.53 (CO). IR (cm^{-1}) 3220 (νNH), 1686 (νCO), 1600 (νCO). FAB$^+$-MS *m*/*z* ($C_{16}H_{24}N_2O_2S_2$, 340): 341 (M + H$^+$).

[15]aneS$_2$ON$_2$–(CH$_2$CONHPh)$_2$ (22). Using the same procedure as outlined for the preparation of **12**, [15]aneN$_2$OS$_2$ (0.192 g, 0.767 mmol) and *N*-phenyl-2-chloroacetamide (0.260 g, 1.53 mmol) afforded 0.23 g (58%) of the product as pale yellow oil after chromatography on silica-60 (dichloromethane –methanol 40 : 1 eluent) and drying under reduced pressure. Anal. calc. for $C_{26}H_{36}N_4O_3S_2 \cdot 0.2CH_2Cl_2$, C, 58.96; H, 6.87; N, 10.50%. Found: C, 59.28; H, 6.64; N, 11.02%. ^{1}H-NMR ($CDCl_3$): δ (ppm) 2.83 (m, 12H, CH_2), 2.96 (m, 4H, CH_2), 3.20 (s, 4H, CH_2), 3.75 (m, 4H, CH_2), 7.07 (t, 2H, Ph), 7.28 (t, 4H, Ph), 7.60 (d, 4H, Ph), 9.29 (br, s, 2H, NH). ^{13}C-NMR ($CDCl_3$): δ (ppm) = 30.09 (CH_2), 32.14 (CH_2), 52.12 (CH_2), 55.10 (CH_2), 60.32 (CH_2), 71.49 (CH_2), 119.40 (C_{quat}), 123.99 (CH), 128.74 (CH), 137.48 (C_{quat}), 168.68 (CO). IR (cm^{-1}) 3300 (νNH), 1678 (νCO), 1598 (νCO). FAB$^+$-MS *m*/*z* ($C_{26}H_{36}N_4O_3S_2$, 516): 517 (M + H$^+$).

[15]aneS$_3$N$_2$–(CH$_2$CONHPh)$_2$ (23). Using the same procedure as outlined for the preparation of **12**, [15]aneN$_2$S$_3$ (0.215 g, 0.807 mmol) and *N*-phenyl-2-chloroacetamide (0.274 g, 1.62 mmol) afforded 0.30 g (70%) of the product as a white solid after washing with acetone and drying under reduced pressure. Anal. calc. for $C_{26}H_{36}N_4O_2S_3$, C, 58.61; H, 6.81; N, 10.52%. Found: C, 58.41; H, 6.52; N, 10.35%. ^{1}H-NMR ($CDCl_3$): δ (ppm) 2.90 (m, 20H, CH_2), 3.24 (s, 4H, CH_2), 7.10 (t, 2H, Ph), 7.32 (t, 4H, Ph), 7.63 (d, 4H, Ph), 9.29 (br, s, 2H, NH). ^{13}C-NMR ($CDCl_3$): δ (ppm) = 31.03 (CH_2), 33.13 (CH_2), 33.20 (CH_2), 52.45 (CH_2), 55.15 (CH_2), 60.00 (CH_2), 119.52 (C_{quat}), 124.43 (CH), 128.96 (CH), 137.62 (C_{quat}), 168.64 (CO). IR (cm^{-1}) 3291 (νNH), 3256 (νNH), 1685 (νCO), 1597 (νCO). FAB$^+$-MS *m*/*z* ($C_{26}H_{36}N_4O_2S_3$, 532): 533 (M + H$^+$).

[15]aneS$_3$N$_2$–CH$_2$CONHPh (24). A solution of *N*-phenyl-2-chloroacetamide (0.295 g, 1.74 mmol) in acetonitrile (30 mL) was added dropwise to a rapidly stirred suspension of K_2CO_3 (0.240 g, 1.74 mmol) in acetonitrile (40 mL) containing [15]aneN$_2$S$_3$ (0.463 g, 0.174 mmol) at 50 °C. After the addition was complete the mixture was stirred at 50 °C overnight and the solvent was evaporated, water added and the products were extracted into dichloromethane and purified by column chromatography on silica-60 (dichloromethane–methanol 14 : 1 eluent) to afford 0.3 g (43%). An analytically pure sample was obtained by recrystallisation from a 1,2-dichloroethane –hexane mixture. Anal. calc. for $C_{18}H_{29}N_3OS_3$, C, 54.10; H, 7.31; N, 10.51%. Found: C, 54.46; H, 7.19; N, 10.12%. ^{1}H-NMR ($CDCl_3$): δ (ppm) 2.83 (m, 20H, CH_2), 3.25 (s, 2H, CH_2), 7.11 (t, 1H, Ph), 7.32 (t, 2H, Ph), 7.72 (d, 2H, Ph), 9.71 (br, s, 1H, NH). IR (cm^{-1}) 3290 (νNH), 3205 (νNH), 1669 (νCO), 1598 (νCO). FAB$^+$-MS *m*/*z* ($C_{18}H_{29}N_3OS_3$, 399): 400 (M + H$^+$).

[Ag([12]aneS$_3$N–CH$_2$CONH-^{t}Bu)(NO$_3$)][Ag(18)(NO$_3$)]. To **18** (0.0233 g, 0.0692 mmol) in dichloromethane (0.5 mL) was added $AgNO_3$ (0.0118 g, 0.0692 mmol) in acetonitrile (1 mL) and the mixture was heated gently until the white precipitate

Table 3 Crystal data and structure refinement

Compound	[12]aneS$_3$N–CONHCOPh (**1**)	[12]aneS$_3$ N–CSNHCOPh (**2**)	[12]ane S$_2$ON–CONHCOPh (**3**)	[12]aneS$_2$ON–CH$_2$ CONHCONH-^{t}Bu (**12**)	[12]aneS$_2$ON$_2$–(CH$_2$CONH CONH-^{t}Bu)$_2$ (**15**)	[15]aneS$_3$N$_2$–(CH$_2$CONHPh)$_2$ (**23**)	[Ag(**18**)(NO$_3$)]
Formula	$C_{16}H_{22}N_2O_2S_3$	$C_{16}H_{22}N_2OS_4$	$C_{15}H_{19}N_3O_3S_2$	$C_{16}H_{22}N_2O_3S_2$	$C_{25}H_{48}Cl_2N_6O_5S_2$	$C_{26}H_{36}N_4O_2S_3$	$C_{14}H_{28}AgN_3O_4S_3$
M	370.54	386.60	363.53	354.48	647.71	532.77	506.44
Crystal system	Triclinic	Monoclinic	Monoclinic	Monoclinic	Triclinic	Monoclinic	Monoclinic
Space group	$P\bar{1}$	$P2_1/c$	$P2_1/c$	$P2_1/c$	$P\bar{1}$	$P2_1/n$	$P2_1/c$
a/Å	9.4753(10)	13.450(3)	12.5943(8)	5.4621(4)	10.3080(7)	17.049(3)	11.967(2)
b/Å	12.7836(13)	7.195(2)	14.8366(10)	19.6240(14)	10.3129(7)	10.189(2)	20.985(4)
c/Å	15.653(2)	20.096(4)	10.1311(7)	16.0384(12)	16.9116(11)	17.316(3)	7.750(2)
α/°	73.346(2)	90	90	90	88.351(1)	90	90
β/°	81.158(2)	106.53(3)	99.462(1)	91.023(2)	84.537(1)	115.526(3)	93.036(3)
γ/°	86.034(2)	90	90	90	72.061(1)	90	90
V /Å^3	1794.3(5)	1864.3(5)	1867.3(4)	1718.9(4)	1702.6(3)	2714(2)	1943.5(7)
Z	4	4	4	4	2	4	4
T/K	150(2)	150(2)	150(2)	150(2)	150(2)	150(2)	150(2)
μ(Mo-K_α)/mm^{-1}	0.423	0.514	0.302	0.325	0.354	0.304	1.384
Reflections collected	10 218	4071	11 916	17 134	17 399	24 574	15 778
Unique reflections, R_{int}	7810, 0.041	3666, 0.033	4539, 0.030	4171, 0.034	7793, 0.016	6866	4691, 0.044
R_1	0.0542 [3814, $I > 2\sigma(I)$]	0.0364 [3153, $I > 2\sigma(I)$]	0.0371 [3131, $I > 2\sigma(I)$]	0.0355 [3044, $I > 2\sigma(I)$]	0.0595 [5620, $I > 2\sigma(I)$]	0.0366 [5027, $I > 2\sigma(I)$]	0.0271 [3130, $I > 2\sigma(I)$]
wR_2 [all data]	0.105	0.0878	0.0906	0.0851	0.180	0.101	0.0442

that formed had dissolved. The solution was allowed to cool slowly and yielded the product (0.025 g, 71%) as a white crystalline solid. Crystals suitable for X-ray diffraction were grown by slow diffusion of Et_2O into an acetonitrile solution of [Ag(**18**)(NO_3)]. Anal. calc. for $C_{14}H_{28}AgN_3O_4S_3$, C, 33.20; H, 5.57; N, 8.30%. Found: C, 33.20; H, 5.22; N, 8.08%. ^{1}H-NMR (d^3-MeCN): δ (ppm) 1.30 (s, 9H, CMe_3), 2.86 (s, br, 16H, CH_2), 3.02 (s, 2H, CH_2), 6.53 (br, s, 1H, NH). IR (cm^{-1}) 3282 (νNH), 1657 (νCO), 1560 (νCO). FAB$^+$-MS m/z ($C_{14}H_{28}AgN_2OS_3$, 443): 443 (LAg$^+$).

The synthesis of **25** has been reported previously.[35]

X-ray structure analyses

A summary of the crystal data and refinement parameters for [12]aneS$_3$N–CONHCOPh (**1**), [12]aneS$_3$N–CSNHCOPh (**2**), [12]aneS$_2$ON–CONHCOPh (**3**), [12]aneS$_2$ON–CH$_2$CONH-CONH-^{t}Bu (**12**), [12]aneS$_2$ON$_2$–(CH$_2$CONHCONH-^{t}Bu)$_2$ (**15**),[10] [15]aneS$_3$N$_2$–(CH$_2$CONHPh)$_2$ (**23**) and [Ag(**18**)(NO_3)] is given in Table 3. The crystals were cooled using an Oxford Cryosystems open-flow nitrogen crysostat.[36] Data for **2** were collected on a Stoe Stadi-4 four-circle diffractometer using ω–θ scans while data for **1**, **3**, **12**, **23** and [Ag(**18**)(NO_3)] were collected on a Bruker SMART1000 CCD area detector using ω scans. Data were corrected for Lorentz and polarisation effects and absorption corrections were also applied. The structures were solved by direct methods and subsequent difference-Fourier syntheses.[37,38] All non-H atoms were refined anisotropically[38] and all H-atoms were placed at calculated positions and thereafter refined riding on their parent atoms with U_{iso}(H) = 1.2 U_{eq}(C). CCDC reference numbers 195912 and 607523–607528. For crystallographic data in CIF or other electronic format see DOI: 10.1039/b609180f.

Acknowledgements

We thank the EPSRC and The University of Nottingham for support, and the EPSRC National Mass Spectrometry service at The University of Wales, Swansea for mass spectra. MS gratefully acknowledges receipt of a Royal Society Wolfson Merit Award and of a Royal Society Leverhulme Trust Senior Research Fellowship. LFL acknowledges the Australian Research Council for support.

References

1 (*a*) L. F. Lindoy, *Pure Appl. Chem.*, 1997, **69**, 2179; (*b*) J. R. Price, M. Fainerman-Melnikova, R. R. Fenton, K. Gloe, L. F. Lindoy, T. Rambusch, B. W. Skelton, P. Turner, A. H. White and K. Wichmann, *Dalton Trans.*, 2004, 3715; (*c*) O. Heitzsch, K. Gloe, H. Stephan and E. Weber, *Solvent Extr. Ion Exch.*, 1994, **12**, 475; (*d*) D. Black, A. J. Blake, K. P. Dancey, A. Harrison, M. McPartlin, S. Parsons, P. A. Tasker, G. Whittaker and M. Schröder, *J. Chem. Soc., Dalton Trans.*, 1998, 3953; (*e*) D. Black, A. J. Blake, R. L. Finn, L. F. Lindoy, A. Nezhadali, G. Rougnaghi, P. A. Tasker and M. Schröder, *Chem. Commun.*, 2002, 340; (*f*) J. P. Danks, N. R. Champness and M. Schröder, *Coord. Chem. Rev.*, 1998, **174**, 417; (*g*) A. J. Blake, J. P. Danks, A. Harrison, S. Parsons, P. Schooler, G. Whittaker and M. Schröder, *J. Chem. Soc., Dalton Trans.*, 1998, 2335; (*h*) A. J. Blake, J. P. Danks, I. A. Fallis, A. Harrison, W.-S. Li, S. Parsons, S. A. Ross, G. Whittaker and M. Schröder, *J. Chem. Soc., Dalton Trans.*, 1998, 3969.

2 (*a*) M. M. G. Antonisse and D. N. Reinhoudt, *Chem. Commun.*, 1998, 443; (*b*) P. D. Beer, P. K. Hopkins and J. D. McKinney, *Chem. Commun.*, 1999, 1253.

3 (*a*) D. J. White, N. Laing, H. Miller, S. Parsons, S. Coles and P. A. Tasker, *Chem. Commun.*, 1999, 2077; (*b*) H. A. Miller, N. Laing, S. Parsons, A. Parkin, P. A. Tasker and D. J. White, *J. Chem. Soc., Dalton Trans.*, 2000, 3773; (*c*) P. G. Plieger, P. A. Tasker and S. G. Galbraith, *Dalton Trans.*, 2004, 313; (*d*) S. G. Galbraith and P. A. Tasker, *Supramol. Chem.*, 2005, **17**, 191.

4 (*a*) J. E. Redman, P. D. Beer, S. W. Dent and M. G. B. Drew, *Chem. Commun.*, 1998, 231; (*b*) P. D. Beer and S. W. Dent, *Chem. Commun.*, 1998, 825.

5 (*a*) D. M. Rudkevich, Z. Brzozka, M. Palys, H. C. Visser, W. Verboom and D. N. Reinhoudt, *Angew. Chem., Int. Ed. Engl.*, 1994, **33**, 467; (*b*) D. M. Rudkevich, J. D. Mercer-Chalmers, W. Verboom, R. Ungaro, F. de Jong and D. N. Reinhoudt, *J. Am. Chem. Soc.*, 1995, **117**, 6124.

6 E. A. Arafa, K. I. Kinnear and J. C. Lockhart, *J. Chem. Soc., Chem. Commun.*, 1992, 61.

7 (*a*) M. T. Reetz, C. M. Niemeyer and K. Harms, *Angew., Chem., Int. Ed. Engl.*, 1991, **30**, 1472; (*b*) M. T. Reetz, C. M. Niemeyer and K. Harms, *Angew. Chem., Int. Ed. Engl.*, 1991, **30**, 1474.

8 D. M. Rudkevich, A. N. Shivanayuk, Z. Brzozka, W. Verboom and D. N. Reinhoudt, *Angew. Chem., Int. Ed. Engl.*, 1995, **34**, 2124.

9 J. B. Love, J. M. Vere, M. W. Glenny, A. J. Blake and M. Schröder, *Chem. Commun.*, 2001, 2678.

10 M. W. Glenny, A. J. Blake and M. Schröder, *Dalton Trans.*, 2003, 1941.

11 (*a*) L. G. A. van der Water, W. L. Driessen, M. W. Glenny, J. Reedijk and M. Schröder, *React. Funct. Polym.*, 2002, **51**, 33; (*b*) M. W. Glenny, L. G. A. van de Water, W. L. Driessen, J. Reedijk, A. J. Blake and M. Schröder, *Dalton Trans.*, 2004, 1953; (*c*) M. W. Glenny, L. G. A. van de Water, J. M. Vere, A. J. Blake, W. L. Driessen, J. Reedijk and M. Schröder, *Polyhedron*, 2006, **25**, 599.

12 (*a*) A. J. Blake and M. Schröder, *Adv. Inorg. Chem.*, 1990, **35**, 1; (*b*) S. C. Rawle and S. R. Cooper, *Struct. Bonding (Berlin)*, 1990, **72**, 1; (*c*) J. S. Bradshaw and R. M. Izatt, *Acc. Chem. Res.*, 1997, **30**, 338.

13 (*a*) D. St. C. Black and I. A. McLean, *Aust. J. Chem.*, 1971, **24**, 1401; (*b*) D. S. t. C. Black and I. A. McLean, *Tetrahedron Lett.*, 1969, **45**, 3961; (*c*) S. Shinkai, K. Shigematsu, Y. Honda and O. Manabe, *Bull. Chem. Soc. Jpn.*, 1984, **57**, 2879; (*d*) L. Siegfried and T. A. Kaden, *Helv. Chim. Acta*, 1984, **67**, 29; (*e*) J. Jurczak, S. Kasprzyk, P. Salański and T. Stankiewicz, *J. Chem. Soc., Chem. Commun.*, 1991, 956; (*f*) D. Baldwin, P. A. Duckworth, G. R. Erickson, L. F. Lindoy, M. McPartlin, G. M. Mockler, W. E. Moody and P. E. Tasker, *Aust. J. Chem.*, 1987, **40**, 1861; (*g*) Z. Yang, J. S. Bradshaw, X. X. Zhang, P. B. Savage, K. E. Krakowiak, N. K. Dalley, N. Su, R. T. Bronson and R. M. Izatt, *J. Org. Chem.*, 1999, **64**, 3162; (*h*) R. T. Bronson, J. S. Bradshaw, P. B. Savage, S. Fuangswasdi, S. C. Lee, K. E. Krakowiak and R. M. Izatt, *J. Org. Chem.*, 2001, **66**, 4752; (*i*) M. Tanaka, M. Nakamura, T. Ikeda, K. Ikeda, H. Ando, Y. Shibutani, S. Yajima and K. Kimura, *J. Org. Chem.*, 2001, **66**, 7008.

14 R. B. Bates, K. D. Janda and M. E. Wright, *Acta Crystallogr., Sect. C: Cryst. Struct. Commun.*, 1985, **41**, 263, and references therein.

15 For example see: (*a*) V. Bertolasi, P. Gilli, V. Feretti and G. Gilli, *Acta Crystallogr., Sect. C: Cryst. Struct. Commun.*, 1987, **43**, 1201; (*b*) J. Scheerder, R. H. Vreekamp, J. F. J. Engbersen, W. Verboom, J. P. M. van Duynhoven and D. N. Reinhoudt, *J. Org. Chem.*, 1996, **64**, 3476.

16 (*a*) N. K. Dalley, J. S. Smith, S. B. Larson, K. L. Matheson, J. J. Christensen and R. M. Izatt, *J. Chem. Soc., Chem. Commun.*, 1975, 84; (*b*) N. K. Dalley, S. B. Larson, J. S. Smith, K. L. Matheson, R. M. Izatt and J. J. Christensen, *J. Heterocycl. Chem.*, 1981, **18**, 463; (*c*) R. E. Wolf, Jr, J.-A. R. Hartman, J. M. E. Storey, B. M. Foxman and S. R. Cooper, *J. Am. Chem. Soc.*, 1987, **109**, 4328; (*d*) R. S. Glass, G. S. Wilson and W. N. Setzer, *J. Am. Chem. Soc.*, 1980, **102**, 5068.

17 R. E. DeSimone and M. D. Glick, *J. Am. Chem. Soc.*, 1976, **98**, 762.

18 (*a*) S. E. Hill and D. Feller, *J. Phys. Chem. A*, 2000, **104**, 652, see also; (*b*) R. Blom, D. W. H. Rankin, H. E. Robertson, M. Schröder and A. Taylor, *J. Chem. Soc., Perkin Trans. 2*, 1991, 773.

19 (*a*) A. Furst, R. C. Berlo and S. Hooten, *Chem. Rev.*, 1965, **65**, 51, cautionary note see; (*b*) C. S. Rondestvedt, Jr and T. A. Johnson, *Synthesis*, 1977, 851.

20 For example see: F. D. Bellamy and K. Ou, *Tetrahedron Lett.*, 1984, **25**, 839.

21 For example see: (*a*) T. Endo, H. Tasai, K. Miyazawa, M. Endo, K. Kato, A. Uchida, Y. Ohashi and Y. Yasada, *J. Chem. Soc., Chem. Commun.*, 1983, 636; (*b*) S. V. Kumar and L. M. Rao, *Acta Crystallogr., Sect. B: Struct. Crystallogr. Cryst. Chem.*, 1982, **38**, 974; (*c*) W. B. T. Cruse, *Acta Crystallogr., Sect. B: Struct. Crystallogr. Cryst. Chem.*, 1978, **34**, 2904.

22 (*a*) A. J. Blake, W.-S. Li, V. Lippolis and M. Schröder, *Chem. Commun.*, 1997, 1943; (*b*) M. Munakata, L. Ping Wu, M. Yamamoto, T. Kuroda-Sowa and M. Maekawa, *J. Chem. Soc., Dalton Trans.*, 1995, **1**, 3215; (*c*) M. Fainerman-Melnikova, L. F. Lindoy, S.-Y. Liou, J. C. McMurtrie, N. P. Green, A. Nezhadali, G. Rounaghi and W. N. Setzer, *Aust. J. Chem.*, 2004, **67**, 161.

23 A. J. Blake, N. R. Champness, S. M. Howdle and P. B. Webb, *Inorg. Chem.*, 2000, **39**, 1035.

24 (*a*) J. Clarkson, R. Yagbasan, P. J. Blower, S. C. Rawle and S. R. Cooper, *J. Chem. Soc., Chem. Commun.*, 1987, 950; (*b*) P. J. Blower, J. Clarkson, S. C. Rawle, J. R. Hartman, R. E. Wolf, R. Yagbasan, Jr, S. G. Bott and S. R. Cooper, *Inorg. Chem.*, 1989, **28**, 4040; (*c*) A. J. Blake, R. O. Gould, A. J. Holder, T. M. Hyde and M. Schröder, *Polyhedron*, 1989, **8**, 513.

25 (*a*) A. J. Blake, D. Collinson, R. O. Gould, G. Reid and M. Schröder, *J. Chem. Soc., Dalton Trans.*, 1993, 521; (*b*) A. J. Blake, R. O. Gould, G. Reid and M. Schröder, *J. Chem. Soc., Chem. Commun.*, 1990, 974; (*c*) A. J. Blake, G. Reid and M. Schröder, *J. Chem. Soc., Dalton Trans.*, 1991, 615; (*d*) A. J. Blake, G. Reid and M. Schröder, *J. Chem. Soc., Chem. Commun.*, 1992, 1074; (*e*) A. J. Blake, R. O. Gould, C. Radek and M. Schröder, *J. Chem. Soc., Chem. Commun.*, 1994, 985; (*f*) A. J. Blake, W.-S. Li, V. Lippolis, A. Taylor and M. Schröder, *J. Chem. Soc., Dalton Trans.*, 1998, 2931; (*g*) A. J. Blake, R. O. Gould, W.-S. Li, V. Lippolis, S. Parsons, C. Radek and M. Schröder, *Inorg. Chem.*, 1998, **37**, 5070.

26 T. R. Kelly and M. H. Kim, *J. Am. Chem. Soc.*, 1994, **116**, 7072.

27 P. D. Beer and P. A. Gale, *Angew. Chem., Int. Ed.*, 2001, **40**, 486, and references therein.

28 (*a*) J.-M. Lehn, A. Moradpour and J.-P. Behr, *J. Am. Chem. Soc.*, 1975, **97**, 2532; (*b*) J. D. Lamb, J. J. Christensen, S. R. Izatt, K. Bedke, M. S. Astin and R. M. Izatt, *J. Am. Chem. Soc.*, 1980, **102**, 467; (*c*) J. D. Goddard, *J. Phys. Chem.*, 1985, **89**, 1825.

29 R. Louis, Y. Agnes and R. Weiss, *Acta Crystallogr., Sect. B: Struct. Crystallogr. Cryst. Chem.*, 1977, **33**, 1418.

30 R. Louis, F. Arnaud-Neu, R. Weiss and M. J. Schwing-Weill, *Inorg. Nucl. Chem. Lett.*, 1977, **13**, 31.

31 R. Louis, Y. Agnus and R. Weiss, *Acta Crystallogr., Sect. B: Struct. Crystallogr. Cryst. Chem.*, 1979, **35**, 2905.

32 (*a*) Effendy, R. R. Fenton, L. F. Lindoy, J. R. Price, B. W. Skelton, T. Strixner, G. Wei and A. H. White, *J. Inclusion Phenom.*, 2001, **41**, 185; (*b*) D. Farell, K. Gloe, K. Gloe, G. Goretzki, V. McKee, J. Nelson, M. Nieuwenhuyzen, I. Pal, H. Stephan, R. M. Town and K. Wichmann, *Dalton Trans.*, 2003, 1961.

33 (*a*) A. J. Speziale and L. R. Smith, *J. Org. Chem.*, 1962, **27**, 3742; (*b*) A. J. Speziale and L. R. Smith, *J. Org. Chem.*, 1963, **28**, 1805.

34 P. S. K. Chia, L. F. Lindoy, G. W. Walker and G. W. Everett, *Pure Appl. Chem.*, 1993, **65**, 521.

35 D. Pelissard and R. Louis, *Tetrahedron Lett.*, 1972, **45**, 4589.

36 J. Cosier and A. M. Glazer, *J. Appl. Crystallogr.*, 1986, **19**, 105.

37 G. M. Sheldrick, *SHELXS-97, Program for solution of crystal structures*, University of Göttingen, Germany, 1997.

38 G. M. Sheldrick, *SHELXL-97, Program for refinement of crystal structures*, University of Göttingen, Germany, 1997.